ADVANCED FUNCTIONAL MATERIALS
www.afm-journal.de

Achieving Microparticles with Cell-Instructive Surface Chemistry by Using Tunable Co-Polymer Surfactants

Adam A. Dundas, Valentina Cuzzucoli Crucitti, Simon Haas, Jean-Frédéric Dubern, Arsalan Latif, Manuel Romero, Olutoba Sanni, Amir M. Ghaemmaghami, Paul Williams, Morgan R. Alexander,* Ricky Wildman,* and Derek J. Irvine**

A flow-focusing microfluidic device is used to produce functionalized monodisperse polymer particles with surface chemistries designed to control bacterial biofilm formation. This is achieved by using molecularly designed bespoke surfactants synthesized via catalytic chain transfer polymerization. This novel approach of using polymeric surfactants, often called surfmers, containing a biofunctional moiety contrasts with the more commonly employed emulsion methods. Typically, the surface chemistry of microparticles are dominated by unwanted surfactants that dilute/mask the desired surface response. Time of flight secondary ion mass spectrometry (ToF-SIMS) analysis of particles demonstrates that the comb-graft surfactant is located on the particle surface. Biofilm experiments show how specifically engineered surface chemistries, generated by the surfactants, successfully modulate bacterial attachment to both polymer films, and microparticles. Thus, this paper outlines how the use of designed polymeric surfactants and droplet microfluidics can exert control over both the surface chemistry and size distribution of microparticle materials, demonstrating their critical importance for controlling surface-cell response.

1. Introduction

In the last decade, the use of combinatorial chemistry and high-throughput (HT) screening methods have delivered step-change improvements in the identification and design of new tailored materials.[1–4] In the specific field of biomaterials discovery, HT methods led to the development of bespoke materials for a wide variety of different applications, such as reducing bacterial biofilm formation on medical devices, maintaining stem cell pluripotency, and providing bio-instructive implant materials.[2,4–7] Recent methodological developments have facilitated the screening of a library of (meth)acrylate copolymers to identify a "hit" material that prevented biofilm formation by diverse bacterial pathogens including *Pseudomonas aeruginosa*, *Staphylococcus aureus*, and *Escherichia coli*.[5,8–10] The HT screening method used was based on polymer microarrays and has demonstrated utility for the discovery of biomaterials that have been used as coatings on existing medical devices.[5,10] However, most therapeutic delivery systems are not delivered as coatings, rather they exhibit 3D shapes. Thus, before these new biomaterials can be regarded as potential candidates from which to fabricate medical devices/therapeutic delivery systems, the performance of these copolymers needed to be demonstrated on microparticles to show, for example, that biofilm formation can be controlled in a 3D environment. This is particularly important as topography influences eukaryotic cell and bacterial surface attachment.[11–13] As a consequence, it is important to move from the design of 2D to 3D structures in order to gain a deeper understanding

Dr. A. A. Dundas, V. Cuzzucoli Crucitti, Dr. S. Haas, Prof. R. Wildman, Prof. D. J. Irvine
Centre for Additive Manufacturing
Department of Chemical and Environmental Engineering
Faculty of Engineering
University of Nottingham
Nottingham NG7 2RD, UK
E-mail: Ricky.Wildman@nottingham.ac.uk; Derek.Irvine@nottingham.ac.uk

The ORCID identification number(s) for the author(s) of this article can be found under https://doi.org/10.1002/adfm.202001821.

DOI: 10.1002/adfm.202001821

Dr. A. A. Dundas, Dr. O. Sanni, Prof. M. R. Alexander
Advanced Materials and Healthcare Technologies
School of Pharmacy
University of Nottingham
Nottingham NG7 2RD, UK
E-mail: morgan.alexander@nottingham.ac.uk

Dr. J.-F. Dubern, Dr. M. Romero, Prof. P. Williams
National Biofilms Innovation Centre
Biodiscovery Institute and School of Life Sciences
University of Nottingham
Nottingham NG7 2RD, UK
E-mail: Paul.Williams@nottingham.ac.uk

A. Latif, Prof. A. M. Ghaemmaghami
Division of Immunology
School of Life Sciences
University of Nottingham
Nottingham NG7 2RD, UK

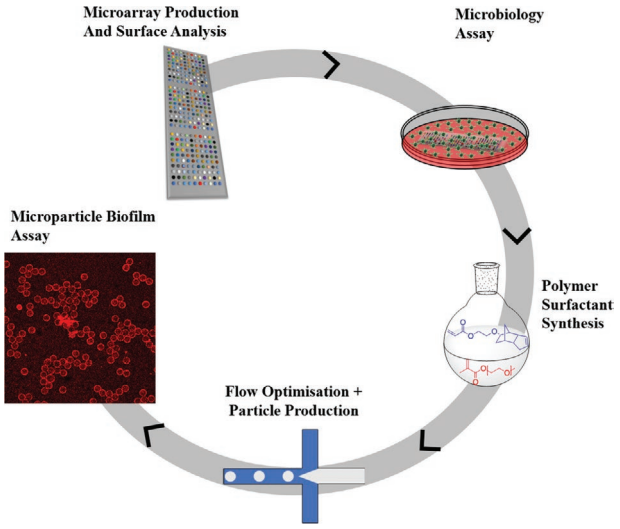

Figure 1. Schematic illustrating the use of polymer microarrays to identify the molecular composition of bespoke polymer surfactants and the subsequent synthesis of surfmers. The surfmers were then used in a flow-focusing microfluidic chip to produce surface-functionalized polymer microparticles. The particles were then incubated with *P. aeruginosa* to determine the impact of the microparticle surface on bacterial attachment and subsequent biofilm formation.

of the interaction of cells with their immediate extracellular environment and, consequently, derive more realistic biological models/assays that mimic real-life conditions.[14] Polymeric microparticles are a simple 3D structure that have numerous healthcare applications including tissue engineering, diagnostics, and drug delivery.[15,16] However, a common problem with the production of particles, regardless of production technique, is the inclusion of unwanted surfactants which cover the surface of particles and are very difficult to remove.[16,17] This presents a problem for biomaterials, as numerous studies have shown that biological-surface interactions are dependent on surface chemistry.[13,16,18,19] For example, the presence of residual surfactant, such as the commonly used poly(vinyl alcohol-co-vinyl acetate) (PVA), has been shown to mask surface chemistry and impact on the resultant bacterial attachment properties[16] Thus, new approaches are required to produce particles which exhibit diverse surface chemistries where the process of preparation does not interfere with surface chemistry.

In this paper, a new strategy for the synthesis of microparticles with specifically selected surface functionality is reported. This consists of the production of bespoke polymer surfmers, that is, amphiphilic surfactants, which possess 3D comb-graft molecular structures. These surfactants are synthesized using monomeric materials that are known to reduce or increase bacterial biofilm formation.[9,10] Monodisperse particle populations were then produced by using droplet-based microfluidics where emulsions were stabilized with the synthesized surfactants (**Figure 1**).

This approach demonstrated that, these surfactants not only aid droplet stabilization but also form an "active", surface located, cell interactive layer because they become entrapped within particle macrostructures as they polymerize. To produce surfactants with controlled molecular weight down to the oligomer level and retain the integrity of chemical functionalities in the polymeric backbone, the efficient, robust and easy scalable catalytic chain transfer polymerization (CCTP) was used as the main polymerization strategy.[20,21] Avoiding the addition of new hetero-functionalities on the polymeric backbone should minimize any undesirable biological consequences from the presence of the surfactant on the particle surface.[22] The surface chemistry of the resultant particles was assessed using time of flight secondary ion mass spectrometry (ToF-SIMS),[3] which demonstrated that the monodisperse polymer particles had been successfully surface functionalized with the desired chemical moieties. In subsequent biological assessment of these particles via incubation with *P. aeruginosa*, it was shown that the polymer microparticles facilitated the desired biological responses in a manner dependent on the surface chemistry of the particles. This response was independent of the materials used to construct particle cores, so correlating with pro- and anti-attachment 2D polymer films.

2. Results and Discussion

By investigating the attachment of *P. aeruginosa* to a wide library of polymers, presented in a microarray format, Sanni et al. found that there was no relationship with water contact angle, but those found to resist biofilm formation were relatively hydrophobic at 80–90 degrees.[5,8,9,23] To form a surfactant, we therefore require a hydrophilic partner for these monomers. Contact printing was used to produce a polymer microarray screen in order to determine the levels of hydrophilic monomer content that could be introduced into a surfactant composition, whilst retaining the desired level of biological performance. Polymer microarrays consisting of 164 copolymer spots were produced with two groups of monomers, one hydrophobic, and one hydrophilic. The array consisted of two different datasets with the first containing two hydrophobic major monomer components with the ability to either prevent (ethylene glycol dicyclopentenyl ether acrylate (EGDPEA)) or support (2-hydroxy-3-phenyoxypropyl acrylate (HPhOPA)) biofilm development (**Figure 2**a). These two monomers were combined with one of the five variable chain length hydrophilic "minor" monomers made from either poly(ethylene glycol) methyl ether methacrylate (mPEGMA) or poly(ethylene glycol) methacrylate (PEGMA) ($PEGMA_{360}$, $PEGMA_{500}$, $mPEGMA_{300}$, $mPEGMA_{500}$, and $mPEGMA_{164}$ (also known as diethylene glycol methyl ether methacrylate)) (Figure 2a). Monomers from the two groups were combined in v:v (hydrophobic:hydrophilic) ratios of 0:100, 50:50, 60:40, 70:30, 75:25, 80:20, 85:15, 90:10, and 100:0. A second set of materials investigated the effect of specific hydrophilic monomer ($mPEGMA_{300}$) concentrations on a range of other biologically active, hydrophobic monomers. In this set, one of ten monomers (phenyl acrylate (PhA), phenyl methacrylate (PhMA), butyl acrylate (BuA), ethyl acrylate (EA), furfuryl methacrylate (FuMA), isobutyl acrylate (iBuA), lauryl acrylate (LaA), tetrahydrofurfuryl acrylate (THFuA), isobornyl methacrylate (IBMA), and 2-*N*-morpholinoethyl methacrylate (NMEMA) were combined pairwise with $mPEGMA_{300}$. These materials were combined in v:v (hydrophobic:$mPEGMA_{300}$) ratios of 0:100, 50:50, 60:40, 70:30, 75:25, 80:20, 85:15, 90:10, and 100:0. $mPEGMA_{164}$ was included as a comparison as

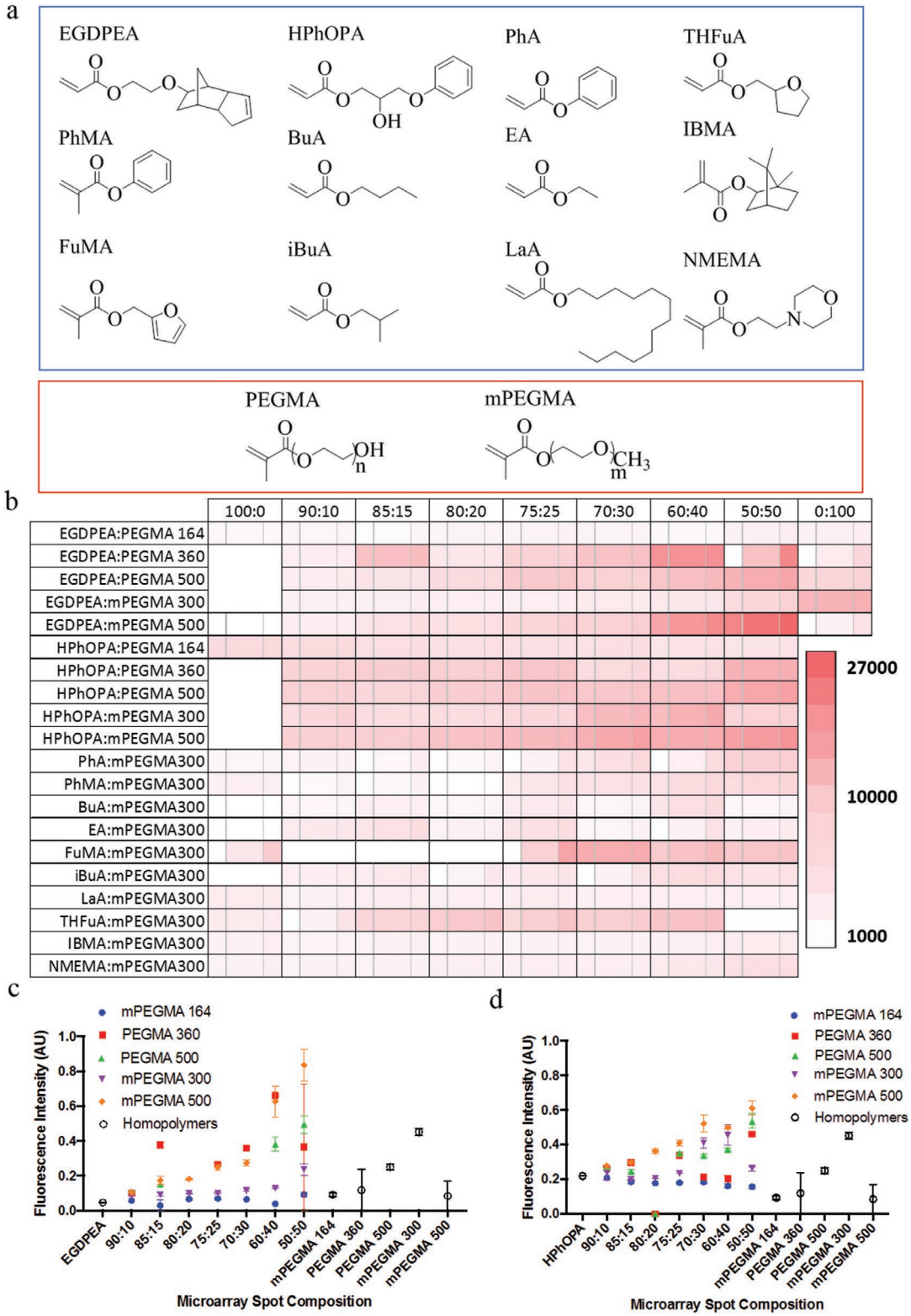

Figure 2. a) Structures of the monomers used for printing polymer microarrays showing major hydrophobic monomers in the blue panel and the minor hydrophilic monomers in the red panel. Chain lengths were either $n = 6$ or 9/10 for PEGMA monomers or $m = 2$, 4/5 or 9/10 for mPEGMA b) results from polymer microarray with mCherry tagged *P. aeruginosa*. Monomer identity is organized into rows and mixing ratio into columns. The center square is the fluorescence value for *P. aeruginosa* attachment (red indicates high biofilm attachment and white indicates low biofilm attachment), while the narrow columns to the left or right indicate ± 1 standard deviation. Data is shown from $n = 6$, $N = 2$ repeats. c) Copolymer data for EGDPEA with a range of different PEG-based hydrophilic chains, showing attachment of *P. aeruginosa* across a sequential copolymer series $n = 6$, $N = 2$ and d) copolymer data for HPhOPA with a range of different PEG-based hydrophilic chains, showing attachment of *P. aeruginosa* across a sequential copolymer series $n = 6$, $N = 2$.

Table 1. Percentage conversions and calculated ratios for synthesized polymer surfactants showing a range of different hydrophilic chains ($PEGMA_{360}$, $PEGMA_{500}$, $mPEGMA_{300}$, and $mPEGMA_{500}$) and also different major co-monomer materials (EGDPEA + HPhOPA).

Entry	Monomers	Conversion[a)] [%]	Feed ratio [%:%]	Actual co-monomer ratio[a)] [%:%]	M_n[b)]	$Đ$[b)]
1	EGDPEA: $PEGMA_{360}$	20	90:10	74:26	24.60	2.90
2	EGDPEA: $PEGMA_{500}$	50	90:10	84:16	304.00	3.50
3	EGDPEA: $mPEGMA_{300}$	43	90:10	87:13	16.00	1.69
4	EGDPEA: $mPEGMA_{500}$	55	90:10	80:20	20.60	1.90
5	HPhOPA: $mPEGMA_{300}$	80	90:10	88:12	26.89	1.86
6	HPhOPA	70	100:0	-	70.00	1.76

[a)]Conversion and actual co-monomer ratio were calculated using ^{1}H-NMR data (Figures S2, S3, and S4, Supporting Information); [b)]M_n and $Đ$ were calculated by GPC.

previously published work showed that copolymers made with five hydrophobic, (meth)acrylate monomers copolymerized with $mPEGMA_{164}$ in mol%:mol% ratio of up to 75:25 could be used as a coating material that retained attachment inhibitory properties at levels comparable with the original homopolymer.[22] Figure 2a,b contain the molecular structures of all monomers used in the study and the HT biological assays of the copolymer spots.

For all copolymer series investigated, the average bacterial attachment deviated from the hydrophobic homopolymer fluorescence value with increasing PEGMA/mPEGMA concentrations in the copolymer (Figure 2c,d). This suggested that the introduction of these hydrophilic co-monomers compromised the biological performance. These results are consistent with the findings upon addition of DEGMA by Adlington et al.[22] Biofilm resistance of weakly amphiphilic (meth)acrylates has been correlated with the hydrophobicity and molecular stiffness of the resultant polymers.[8,9] Dilution of these monomers with PEGMA/mPEGMA is therefore consistent with the increased biofilm formation. When the hydrophilic component is increased beyond a v:v ratio of 90:10, the attachment of *P. aeruginosa* was significantly higher than that of the homopolymer for EGDPEA. However, the EGDPEA-co-$mPEGMA_{300}$ copolymer series exhibited attachment levels that were more consistent with the EGDPEA homopolymer and stayed at within approximately 90% performance up to a v:v ratio of 85:15. Therefore, it was concluded that a hydrophilic chain length of up to 4–5 ethylene glycol units when capped with a methoxy terminal group does not dramatically alter the attachment of *P. aeruginosa* up to a ratio of 85:15. Changes in the bacterial attachment were also observed for the HPhOPA copolymer series containing $PEGMA_{360}$, $PEGMA_{500}$, and $mPEGMA_{500}$ compared to the HPhOPA homopolymer. However, the copolymer series including $mPEGMA_{164}$ and $mPEGMA_{300}$ exhibited attachment levels comparable with the HPhOPA homopolymer. This comparison was also noted in the EGDPEA-co-mPEGMA data suggesting that $mPEGMA_{164}$ and $mPEGMA_{300}$ have not located to the surface, allowing the hit material properties to dominate. Therefore, the v:v ratio 90:10 was selected as the optimum ratio for the surfactant molecular design, as this ratio retained the biological properties of the original homopolymer. Other examples of different copolymers were also included with $mPEGMA_{300}$ only, and these can be found in (Figure S1, Supporting Information).

2.1. Surfactant Synthesis

To synthesize polymeric surfactants which exhibit the target ratio of 90:10 (v:v), the reaction conditions in terms of catalyst concentration (850 ppm) and solvent:co-monomer ratio (3:1 v:v) were maintained constant throughout the polymerizations. The bis[(difluoroboryl)diphenylglyoximato]cobalt(II) (PhCoBF) concentration has been optimized in order to produce materials with M_n's in the range of 15–25 kDa. This M_n range was chosen in order to maintain the viscosity of copolymer solutions used in the microfluidics apparatus within the operating parameters of the equipment. Meanwhile, the 3:1 solvent ratio was selected based on a previous study on EGDPEA:$mPEGMA_{164}$ copolymerization, where this ratio was found to deliver the best results for achieving the target co-monomer ratio, controlling M_n, and polydispersity.[22] However, for HPhOPA based surfactants, a higher solvent:co-monomer ratio (5:1 (v/v)) was used because of the high viscosity exhibited by the starting materials. The percentage conversions and the molecular weights of the copolymer library generated in this study are shown in **Table 1**.

The data in Table 1 shows that all the M_n's are in the target range except EGDPEA-*co*-$PEGMA_{500}$ (Table 1 entry 2) which exhibited higher M_n and $Đ$ (304 kDa and 3.50). It was also observed that EGDPEA-*co*-$PEGMA_{360}$ (Table 1 entry 1) exhibited a significantly higher $Đ$ and lower conversion than the $mPEGMA_{300}$ copolymer (Table 1 entry 3). This was attributed to a negative interaction between the CCTP catalyst and the hydroxy end-group of PEGMA. The presence of electronic substituents, such as free −OH or free amino groups, in the monomer structure can inhibit the catalytic activity by not allowing the release of the cobalt complex from the transition state, as Biasutti et al. have demonstrated.[24] In particular, when mPEGMA (300 and 500 Da) was used as the hydrophilic counterpart, improvements were observed, in both of the copolymers, with either higher conversion or achieving the target M_n with a smaller polydispersity (aligned with Free Radical Polymerisation values). The copolymer bearing the methoxy equivalent of $PEGMA_{360}$ ($mPEGMA_{300}$), (Table 1 entry 3), showed a conversion more than double (43%) that of the 20% of EGDPEA-co-$PEGMA_{360}$ as well as a reduction in M_n and $Đ$. Despite the similar conversion between EGDPEA-*co*-$mPEGMA_{500}$ and EGDPEA-co-$PEGMA_{500}$, the EGDPEA-*co*-$mPEGMA_{500}$ result confirmed the greater compatibility of mPEGMA with the CCTP mechanism as the products exhibited a decreasing of the M_n, from 304 to 20 kDa. This was

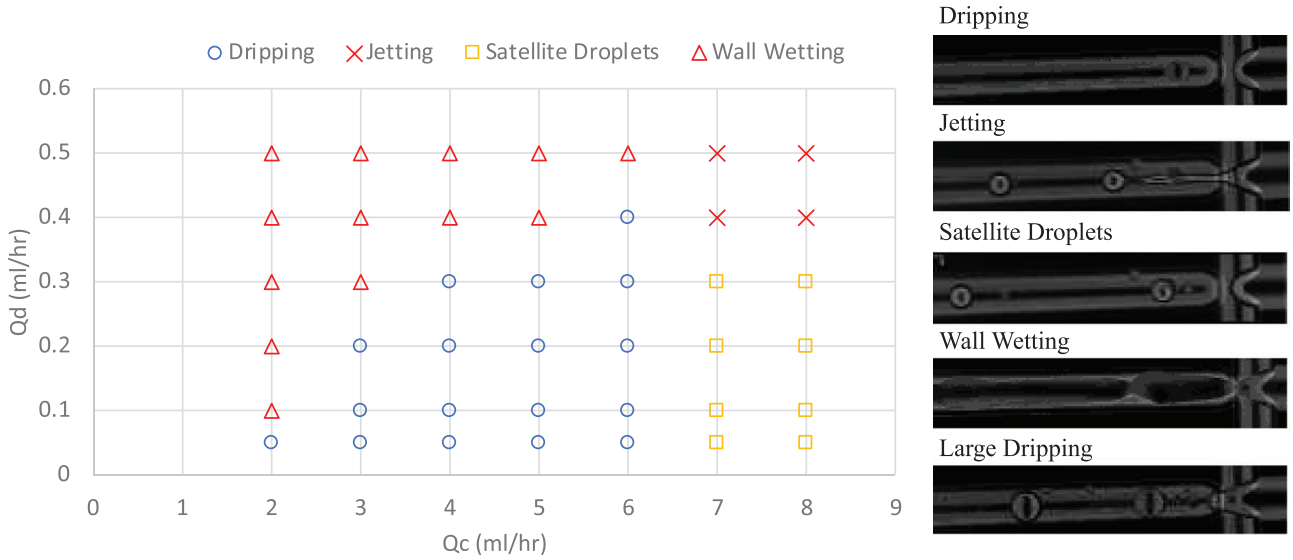

Figure 3. Flow diagram of an oil-in-water microfluidics system with HMDA core material and EGDPDEA-co-mPEGMA$_{300}$. O denotes idealistic dripping behavior, X denotes jetting behavior, ϒ denotes formation of satellite droplets, and Δ denotes flow rates which caused wall wetting events. Blue denotes region of flow rates that produces monodisperse emulsions, red denotes areas of no emulsion formation, and orange denotes area which produces variable emulsion sizes. Images show examples of dripping, jetting, satellite droplet formation, and wall wetting events respectively.

also confirmed through a reduction in polydispersity from 3.5 to 1.9. Therefore, the presence of a methoxy end-group on the side chain of the hydrophilic PEG-based co-monomer resulted in greater control. For HPhOPA, the conversion achieved was ≈80% and the M_n was slightly higher than the targeted range (26.89 kDa). The higher M_n obtained, compared to the target of 20 kDa or below, was attributed to the presence of a hydroxy group in the HPhOPA side chain which may interfere with the catalyst action, a conclusion supported by the much higher M_n achieved for the CCTP-produced HPhOPA homopolymer (Table 1, Entry 6) . However, it was hypothesized that this −OH group will not be as available to interact with the catalyst as in the case of PEGMA, due to the presence of a bulky phenyl group which will give the pendant group a rigid conformation and so restricted flexibility.

The co-monomer ratio achieved within the polymer backbone was determined by ^{1}H-NMR analysis of the purified copolymers. The results in Table 1 show that the final monomer composition of all the surfactants was close to the target feed mol:mol ratio of 90:10 and within a range from 80:20 to 88:12. These results showed that the mPEGMA$_{300}$ co-polymer gave ratios that were closer to the target value of 90:10 determined by the polymer microarray screening results compared to the mPEGMA$_{500}$ alternative. Thus, this synthetic route successfully generated polymeric surfactants with chemical compositions similar to those used for the 2D screen for the bacterial attachment. It also highlighted the use of mPEGMA$_{300}$ for the on-going surfactant design to provide an optimal biological response because it delivers copolymers of target structure, a higher conversion compared with the PEGMA copolymers and gives the target value of copolymer ratios. This synthesis could be developed further through high throughput methods to manufacture many functionalized surfactants with the mPEGMA$_{300}$ comonomer.[25]

2.2. Microparticle Production

To determine the suitability of mPEGMA$_{300}$ based surfactants for microfluidic production of microparticles, the polymers were used as surfactants in an oil-in-water (O/W) droplet flow-focusing system. The dispersed phase which was fed into the center channel consisted of 97% 1,6 hexanediol diacrylate (HMDA) as the particle "core" material, 2% (w:v) polymer surfactant and 1% (w:v) photoinitiator (2,2-Dimethoxy-2-phenylacetophenone (DMPA)). The continuous phase used was distilled water, which was fed into two side channels located perpendicular to the central feed. The emulsion droplets formed by impinging these two phases were collected in a receiver flask where they were irradiated with a 365 nm fiber optic UV source to form solid polymer microparticles. The flow of both the continuous and dispersed phase was optimized to ensure that particles were produced, whilst reducing the risk of wall-wetting events, jetting behavior and unstable particle formation. **Figure 3** shows the flow diagram of the system using the EGDPEA-*co*-mPEGMA$_{300}$ surfmer.

As shown in Figure 3, the EGPDEA-*co*-mPEGMA$_{300}$ surfactant was sufficiently amphiphilic to produce stable emulsions. As the flow rates of both the continuous (Q_c) and dispersed phases (Q_d) increased, the system started to display jetting behavior, while an increase in Q_c alone resulted in the appearance of satellite droplets. However, if the dispersed flow rate is not large enough, the size of the emulsions formed begins to increase and this leads to wall-wetting events. Therefore, the conditions of Q_c = 5 mL h^{-1} and Q_d = 0.2 mL h^{-1} were chosen as flow rates that would ensure the long-term stability of emulsion production within the microfluidics system whilst maximizing particle output. The effect of the PEGMA/mPEGMA chain length on the emulsion/particle stability was investigated, and SEM images in Figure S5, Supporting Information show that

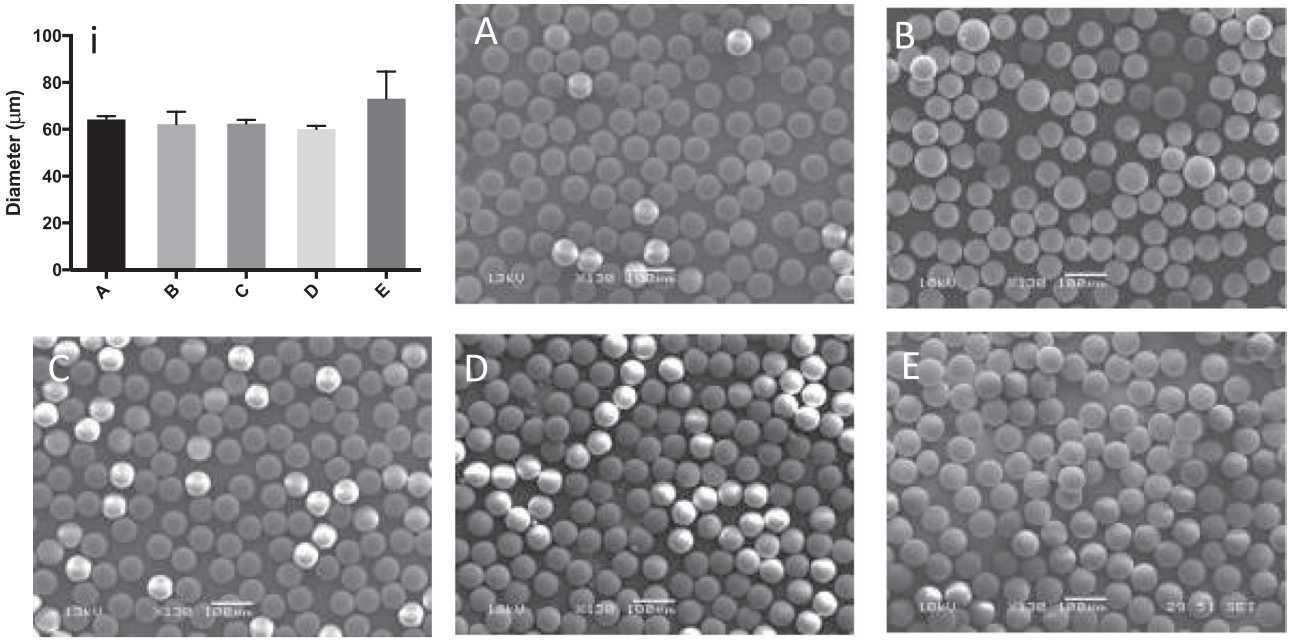

Figure 4. SEM images of polymer microparticles produced using a microfluidic droplet approach. (i) size of particles shown in images A–E. A) Monodisperse particles made with EGDPEA-co-mPEGMA$_{300}$ surfactant with a core made from HMDA and a size of 64.30 ± 1.33 µm (CV = 2.1%). B) Particles made with EGDPEA-*co*-mPEGMA$_{300}$ and HPhOPA-*co*-mPEGMA$_{300}$ in a 1:1 ratio with a core made from HMDA and a size of 62.2 ± 5.2 µm (CV = 8.4%). C) Particles produced with HPhOPA-co-mPEGMA$_{300}$ with a core made from HMDA with a size of 62.42 ± 1.66 µm (CV = 2.7%). D) Particles made with PVA surfactant with a core made from HMDA with a size of 61.60 ± 2.93 µm (CV = 4.8%). E) Particles made with only HMDA core material with no surfactant with a size of 73.09 ± 11.63 µm (CV = 15.9%).

there was little effect on the particle polydispersity. Therefore, the hydrophilic component mPEGMA$_{300}$ was selected as the co-monomer for the rest of the study based on the conclusions derived from the synthesis and manufacturing data, as well as from the 2D biological screening assay.

Prior to collecting particles with the HPhOPA-co-mPEGMA$_{300}$ surfactant, a flow diagram was constructed (Figure S6, Supporting Information). Particles were produced using the HPhOPA-co-mPEGMA$_{300}$ polymer to observe whether monodisperse particles could be produced with surfactants made from different monomers. A 1:1 wt:wt ratio of EGDPEA-*co*-mPEGMA$_{300}$ and HPhOPA-*co*-mPEGMA$_{300}$ was also used to determine whether the polymer surfactant could be blended to create stable particles with a cofunctionalized surface. The microfluidics particle sizing data obtained are shown in **Figure 4**.

The production of polymer microparticles using droplet microfluidics generated monodisperse particle populations with individual surfactants (Figure 4a–c). When no surfactant was added, the HMDA core monomer was sufficiently amphiphilic to be able to produce polymer microparticles, but with a much broader size distribution (CV = 15.9%). Additionally, Figure 4b shows that it is possible to produce particles when incorporating two different surfactants within the production method, where both EGDPEA-*co*-mPEGMA$_{300}$ and HPhOPA-*co*-mPEGMA$_{300}$ were used at a ratio of 1:1 wt:wt and an overall 2% wt:wt surfactant concentration. However, the size distribution was slightly larger (CV = 8.4%) when compared to that obtained using EGDPEA-*co*-mPEGMA$_{300}$ or HPhOPA-*co*-mPEGMA$_{300}$ alone (CV = 2.1 and 2.7% respectively). This process could be particularly useful when wanting to cofunctionalize particles with different biological properties for an application such as wound healing where it is desirable to promote an appropriate immune response whilst preventing bacterial biofilm formation.

2.3. Microparticle Surface Characterization

Time of flight secondary ion mass spectrometry (ToF-SIMS) analysis was conducted to investigate the surface chemistry of the microparticles produced. Data was collected in both positive and negative secondary ion mode in order to determine unique ions associated with the polymer surfactants. Unique identifiers for EGDPEA ($C_5H_7^+$), HPhOPA ($C_6H_5O^-$), and mPEGMA$_{300}$ ($C_3H_7O^+$) were identified for each surfactant. No characteristic peak could be identified for the HMDA core polymer. However, particles prepared with surfactant were compared with the HMDA core particles prepared without surfactant, shown in Figure 4e, to demonstrate the difference between the unfunctionalized and functionalized particles. Flat controls of both EGDPEA-*co*-mPEGMA$_{300}$ and HPhOPA-*co*-mPEGMA$_{300}$ were used to highlight any molecular level differences in the surface conformations introduced by moving from flat to particle surfaces (**Figure 5**).

Microparticles made with only EGDPEA-*co*-mPEGMA$_{300}$ or HPhOPA-*co*-mPEGMA$_{300}$ only generated one unique ions ($C_5H_7^+$ or $C_6H_5O^-$) to show the presence of either EGDPEA or HPhOPA on the particle surface. Comparison of the particles with the plain core HMDA particles clearly demonstrated that the ions were unique to the two individual surfactants and therefore showed that the surfactant is located at the surface of

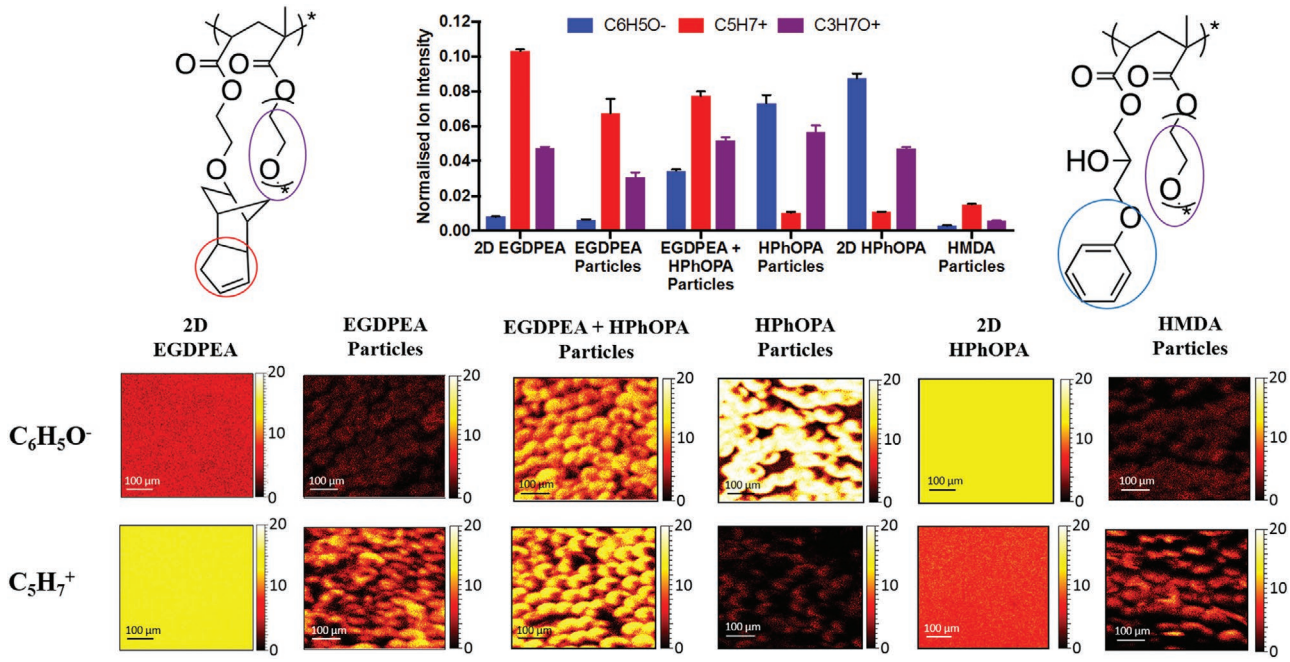

Figure 5. ToF-SIMS data showing intensities of 3 key ions associated with 3 monomers within the surfactant structures ($C_5H_7^+$ – EGDPEA, $C_6H_5O^-$ – HPhOPA and $C_3H_7O^+$ – mPEGMA) where the ions from the structures are circled in red, blue, and purple respectively. Samples (from left to right) include: 2D EGDPEA-co-mPEGMA$_{300}$ sample spun cast onto silicon wafer, microparticles made using EGDPEA-co-mPEGMA$_{300}$ surfactant, microparticles made using both EGDPEA-co-mPEGMA$_{300}$ and HPhOPA-co-mPEGMA$_{300}$ polymer surfactant, particles made from HPhOPA-co-mPEGMA$_{300}$ polymer surfactant, a 2D HPhOPA-co-mPEGMA$_{300}$ sample spun cast onto silicon wafer and microparticles made using no surfactant and only the core material HMDA. Ion images for $C_6H_5O^-$ and $C_5H_7^+$ below the graph correspond directly to the samples on the graph.

the particles. This process ensured that the surface was functionalized with the biologically active material of choice. By using both surfactants in a microparticle batch production it was also possible to show that both $C_5H_7^+$ and $C_6H_5O^-$ ions are present on the particle surface, indicating that surfaces with mixed surfactants had been successful produced. The ion indicative of the mPEGMA chain ($C_3H_7O^+$) can also be found at the surface of the functionalized particles. However, the intensity for this ion is reduced on the HMDA core particle with no surfactant, which is to be expected as there is no mPEGMA on the sample and therefore a reduced $C_3H_7O^+$ intensity. These results establish the concept that, by using bespoke functionalized surfactants, polymer microparticles can be manufactured with specific targeted surface chemistry functionalization. Therefore, such particles should allow for specific surface chemistry structures to be tested on a 3D scale that was not previously possible.

2.4. Cell Cytotoxicity and Bacterial Attachment to Polymer Microparticles

Only trace amounts of monomer were detected using an NMR extraction process in chloroform (Figure S7, Supporting Information). To ensure that cells remain viable during particle exposure, cytotoxicity tests with MRC-5 (ATCC CCL171) human lung fibroblasts were performed and showed no cytotoxicity up to 5 mg mL^{-1} (Figure S8, Supporting Information). This demonstrated that any small traces of monomer did not affect the cell viability. To observe whether the surfactant surface chemistry had an effect on biological performance, particles were cultured with fluorescently labelled *P. aeruginosa* in RPMI medium for 24 h. Data was acquired using confocal microscopy to measure fluorescence. The analysis of attachment/biofilm levels was performed using a computer script that discarded any background fluorescence and only measured fluorescence associated with the particles by using both the brightfield and fluorescence images. The data was normalized for surface area and to the non-surfactant HMDA control for comparative purposes (**Figure 6**).

The variation in biological performance related to modifying the surface chemistry via the choice of surfactant used is exemplified in the data presented in Figure 6. This figure shows how the expected HPhOPA-based surfactant exhibited an increase in biofilm formation compared with the EGDPEA and no surfactant (HMDA) control samples (2.2 and 1.3-fold respectively). In order to confirm that the variation in biological performance of 3D particles could be attributed directly to the surface chemistry, rather than the 3D topography of the particles, a series of 2D films of the homopolymers of EGDPEA and HPhOPA were prepared and a *P. aeruginosa* attachment/biofilm assay was carried out (Figures S9–10, Supporting Information). These results show how (meth)acrylate polymers modify the behavior of bacteria on surfaces; both on individual particle surfaces as well as a coating as previously demonstrated.[10,22] This also provides evidence that these (meth)acrylate polymers, when incorporated into surfactants, can be used to functionalize surfaces with a unimolecular coating, which would be impossible with the original homopolymer. It also extends the utility of polymers

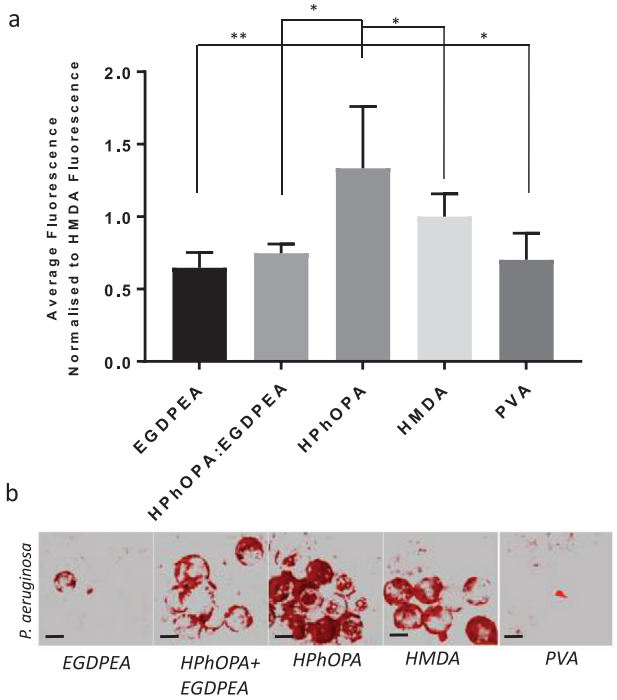

Figure 6. a) Surface coverage by single species (*P. aeruginosa*) biofilms quantified after 24 h incubation on particles coated with EGDPEA, HPhOPA+EGDPEA, HPhOPA, none, and PVA surfactants respectively in RPMI. Quantification was performed on fluorescence images acquired from a 48 well-plate considering an area of 568 × 568 µm. Error bars equal ± 1 SD unit, $n = 3$. Particle data were normalized for surface area and then to the non-surfactant (HMDA) control for comparison. b) Confocal microscopy images for mCherry tagged *P. aeruginosa* growing on each polymer surface. Each image is 295 × 295 µm.

discovered through the polymer microarray platform beyond currently used dip-coating applications.[26] This will therefore enable the targeting of further biofilm prevention applications where a dip-coating procedure would be inappropriate, such as for preventing infections in wounds where particles would offer a better packing density. This method of delivery would also have potentially lower associated costs by reducing the quantity of expensive bioactive polymers as consequence of only using minimal material (2%) as a surfactant in a microfluidic setup. PVA was also shown to prevent biofilm formation on the surface effectively, and this corresponds with previous literature.[16,27] This data demonstrates the dependence of biological performance on the surface chemistry of the 3D particles and therefore the importance of controlling surface chemistry by using specific comb-graft surfactants.

3. Conclusion

In conclusion, this work has demonstrated that functionalized comb-graft surfactants can be synthesized via CCTP with a target hydrophobic: hydrophilic monomer content. These surfactants have been used to stabilize 1.6 hexanediol diacrylate emulsions in water with a flow-focusing microfluidic technique to produce monodisperse polymer microparticles. The functionalization of the particles was confirmed by using ToF-SIMS which demonstrated the presence of key ions on the surface of particles compared to microparticles that had been prepared without any surfactant. The importance of this surfactant layer was shown by the incubation of the polymer microparticles with fluorescently labelled *P. aeruginosa* over 24 h, which showed a clear difference in biofilm formation which was dependent on particle surface chemistry. This work demonstrates the advantageous use of entrapped surfactants for surface-cell interactions, opening new opportunities and applications for 3D biomaterials, including wound healing, injectable therapeutics and for influencing stem cell differentiation.

4. Experimental Section

Materials: All the materials were used as received unless stated otherwise. Ethylene glycol dicyclopentenyl ether acrylate (EGDPEA), 2-hydroxy-3-phenoxypropyl acrylate (HPhOPA), Poly(ethylene glycol) methacrylate with an average M_n of both 360 and 500 ($PEGMA_{360}$ and $PEGMA_{500}$) and Poly(ethylene glycol) methyl ether methacrylate with an average M_n of 164, 300, and 500 ($mPEGMA_{164}$, $mPEGMA_{300}$, and $mPEGMA_{500}$) were purchased from Sigma-Aldrich. 2, 2′-azobis (2-methylpropionitrile) (AIBN, 98%) and 1,6 hexanediol diacrylate (HMDA, 80%) were also obtained from Sigma-Aldrich. The catalytic chain transfer agent Bis[(difluoroboryl) diphenylglyoximato] cobalt (II) (PhCoBF) was supplied from DuPont. The cyclohexanone and heptane used as solvents in synthesis and precipitation, respectively, were used as received and supplied by Scientific Laboratory Supplies and VWR Chemicals, respectively.

Polymer Microarray Production: Slides were prepared by dip-coating epoxy-coated glass slides (Genetix) into a 4% (w/v) poly(hydroxyethyl methacrylate) solution in ethanol. Slides were left to dry in ambient conditions for 24 h. Polymer microarrays were formed using a XYZ3200 dispensing workstation (Biodot) at 25 °C, 30–40% humidity, and less than 0.2% O_2 levels. Quilled metal pins (946MP6B, Arrayit) were used to transfer monomer solutions (with 1% (w/v) photoinitiator (2,2 dimethoxy-2-phenylacetonphenone)) onto 20 pHEMA-coated slides and irradiated with UV light.[28,29] Microarray slides were allowed to dry for a week under vacuum to remove residual solvents and any trace of unreacted monomer before bacterial assays.[28]

Bacterial Strains and Growth Conditions: *P. aeruginosa* strain PAO1 (Washington sub-line, Nottingham collection) was routinely grown at 37 °C in lysogeny broth (LB) with shaking at 200 rpm or on LB agar (2% w/v). Plasmids for constitutively expressing the fluorescent protein mCherry (pMMR)[30] were introduced into the host strain by conjugation.

Polymer Microarray 2D Biological Assay: Before microarrays were incubated with *P. aeruginosa*, the slides were UV sterilized for 10 min. After sterilization, slides were placed in 15 mL of RPMI-1640 medium in a petri dish which was inoculated (OD_{600} = 0.01) with mCherry tagged *P. aeruginosa* and left for 24 h at 37 °C at 60 rpm shaking. These conditions result in a continuous flow over the surface. After incubation, slides were twice washed with phosphate-buffered saline at room temperature for 5 min and rinsed with distilled water. Fluorescence images were taken of both the control slide and bacteria-probed slide using a GenePix Autoloader 4200AL (Molecular Devices, US) scanner using a 655–695 nm filter. The fluorescence signal from the bacteria attached to polymer spots was acquired by subtracting the fluorescence of the control slide from the fluorescence of the slide incubated with bacteria, which directly correlates with biofilm formation on the polymer surface.

Copolymer Surfactant Synthesis: A typical protocol used for the catalytic chain transfer polymerization (CCTP) of both EGDPEA-*co*-PEGMA360, EGDPEA-*co*-mPEGMA300, and HPhOPA-*co*-mPEGMA300 copolymers was as follows. The appropriate quantities of the monomers required to reach the targeted molar ratios (EGDPEA:$PEGMA_{360}$ 2.15 g:0.35 g; EGDPEA:$PEGMA_{500}$/$mPEGMA_{500}$ 2.04g:0.47 g; EGDPEA:$mPEGMA_{300}$ 2.06 g:0.44 g; HPhOPA:$mPEGMA_{300}$ 2.11 g:0.33 g), were dissolved in cyclohexanone in a 1:3 v/v ratio. Initiator and transfer agents were added

in the reaction vessel with monomers and solvents in the follow order. A PhCoBF stock solution of 5 mg mL^{-1} was prepared in cyclohexanone from which aliquot was taken in order to achieve the final concentration of 850 ppm (0.89 mg mL^{-1}). Finally, AIBN (0.5% wt/wt with respect to the monomers) was dissolved in cyclohexanone and degassed separately prior to being added to the reaction mixture. Finally, the reaction vessel and the AIBN solution were degassed purging argon using a standard Shlenk line technique for at least 2 h. The temperature adopted during the reaction was 75 °C for 18 h. Polymer purification was conducted in excess heptane. The usual non-solvent:reaction media ratio was 5:1 v/v in order to enhance the precipitation process and, finally, the precipitated materials were collected in a vial and left in a vacuum oven for at least 24 h.

NMR spectroscopic analysis was performed on the crude polymerization solution to determine polymer conversion and, finally, on the precipitate to establish the actual monomer ratio of the final copolymer composition.[31] To evaluate the molecular weight of the materials, the purified samples were dissolved in HPLC grade THF for GPC analysis.

^{1}H-Nuclear Magnetic Resonance Analysis: ^{1}H NMR spectra were recorded at 25 °C using a Bruker DPX-300 spectrometer (400 MHz). Chemical shifts were recorded in δH (ppm). Samples were dissolved in deuterated chloroform ($CDCl_3$) to which chemical shifts are referenced (residual chloroform at 7.26 ppm). The ^{1}H NMR spectra of the EGDPEA monomer (400 MHz, $CDCl_3$, δH ppm): 6.30 (^{1}H, HCH = CH, dd), 6.03 (^{1}H, CH_2=CH,m), 5.70 (^{1}H, HCH=CH,dd), 5.45 (^{1}H, dicyclopentenyl CH=CH, m), 4.14 (^{2}H, O−CH_2CH_2,m), 3.5 (^{2}H,CH_2CH_2O,m), 3.34 (1H, O−CH−(C_9H_{12}),m), 2.46–2.29 (m, C_7H_{10}), 2.11–1.72 (m, C_7H_{10}), 1.51–1.09 (m, C_7H_{10}).

The ^{1}H NMR spectra of the PEGMA monomer (400 MHz, $CDCl_3$, δH ppm): 5.81 (^{1}H, HCH=CH_3, s), 5.27 (^{1}H, HCH=CH_3, s), 3.97 (^{2}H, OCH_2CH_2, m), 3.33 (^{2}H, C=OOCH_2CH_2O, and (OCH_2CH_2O)5, m), 1.71 (^{3}H, CH_2=CH_3, s).

The ^{1}H NMR spectra of the mPEGMA monomer (400 MHz, $CDCl_3$, δH ppm): 5.81 (^{1}H, HCH=CH_3, s), 5.27 (^{1}H, HCH=CH_3, s), 3.97 (^{2}H, OCH_2CH_2, m), 3.43 (^{17}H, C=OOCH_2CH_2O, and (OCH_2CH_2O)5, m), 3.14(^{3}H, OCH_3, s), 1.71 (^{3}H, CH_2 =CH_3, s).

The ^{1}H NMR spectra of the HPhOPA monomer (400 MHz, $CDCl_3$, δH ppm): 7.28–6.91 (^{5}H, C_5H_5, m), 6.41 (^{1}H, HCH=CH_3, s), 6.13 (^{1}H, HCH=CH_3, s), 5.86 (^{1}H, HCH=H, s), 4.61–3.66 (5H, OCH_2HOHCH_2O, m).

The ^{1}H NMR of the EGDPEA:PEGMA copolymer purified (400 MHz, d-Chloroform, δ, ppm): 5.69–5.47 (^{2}H, CH=CH, m), 4.36 (^{4}H, OCH_2CH_2, m), 3.73–3.45 (^{24}H, $CH_2CH_2OCH_2$, CH_2CH_2O of both the monomers along the ester chain and $OCHC_9H_{12}$, m), 2.51–0.95 (10H, C_7H_{10}, m).

The ^{1}H NMR of the EGDPEA: mPEGMA copolymer purified (400 MHz, d-Chloroform, δ, ppm): 5.69–5.47 (2H, CH=CH, m), 4.36 (^{4}H, OCH_2CH_2), 3.73–3.45 (^{20}H, $CH_2CH_2OCH_2$, CH_2CH_2O of both the monomers along the ester chain and $OCHC_9H_{12}$, m), 3.40 (^{3}H, OCH_3, m), 2.51-0.95 (^{10}H, C_7H_{10}, m).

The ^{1}H-NMR of HPhOPA:mPEGMA copolymer purified (400 MHz, d-Chloroform, δ, ppm): 7.22–6.87 (^{5}H, C_5H_5, m), 4.49-3.71 (^{7}H, OCH_2HOHCH_2O, and OCH_2CH_2, 3.61 (^{16}H, CH_2CH_2O OCH_2CH_2O, m), 3.40 (^{3}H, OCH_3, m),

Gel Permeation Chromatography Analysis: GPC analysis was performed by using an Agilent 1260 Infinity instrument equipped with a double detector with the light scattering configuration. two mixed columns at 25 °C were employed, using THF as the mobile phase with a flow rate of 1 mL min^{-1}. GPC samples were prepared in HPLC grade THF and filtered previous injection. Analysis was carried out using Astra software. The number average molecular weight (M_n) and polydispersity ($Đ$) were calculated using PMMA for the calibration curve.

Microfluidic Microparticle Production: Polymer microparticles were produced using a 100 µm hydrophilic 3D flow-focusing microfluidic droplet generator. Two Havard Instrument syringe pumps were used to deliver the continuous and dispersed flows to the microfluidic generator. The continuous phase used was distilled water and was set at a flow rate of 5 mL h^{-1}. The dispersed phase contained the monomer (1,6 hexanediol diacrylate) with 2% w/v polymer surfactant and 1% w/v photoinitiator (2,2 dimethoxy-2-phenylacetophenone) and was set at a flow rate of 0.2 mL h^{-1}. Emulsions were then collected in distilled water and irradiated with UV radiation at 365 nm. Particles were then characterized for size by using scanning electron microscopy and analyzed using ImageJ.

Microparticle Surface Characterisation: Microparticles were placed onto a poly(hydroxyethyl) methacrylate substrate and subjected to mass-spectrometry using a ToF-SIMS IV (IONTOF GmbH, Münster, Germany) instrument. 500 µm × 500 µm scans were taken with a Bi^{3+} primary ion source. Data were calibrated and analyzed using IonToF software.

Cell Culture: The human lung fibroblasts MRC-5 (ATCC CCL171, ATCC) were cultured in MEM Eagles (Sigma) supplemented with fetal bovine serum (10%, Sigma), L-glutamine, non-essential amino acids, penicillin/streptomycin, and sodium pyruvate (1% each, Sigma). The cells were cultured in T75 flasks at 37 °C with 5% supplemental CO2 until 90% confluent, before passaging.

Cytotoxicity Assay: After 24 h of the culture period, a two-color fluorescence cell viability assay based on simultaneous determination of live and dead cells by calcein-AM and ethidium homodimer-1 was used. The assay was performed by incubating cells in PBS supplemented with 4 µM calcein-AM and 2 µM ethidium homodimer-1 (LIVE/DEAD viability/cytotoxicity kit, Invitrogen) at 37 °C for 20 min. After which, the cells were washed thrice with fresh PBS and imaged. The emitted fluorescent signals of calcein-AM and ethidium homodimer were collected at 517 and 615 nm, respectively. Fibroblasts were considered viable if the cytoplasm was with calcein-AM (green) and if chromatin was not labelled with ethidium homodimer-1 (red).

Bacterial Biofilm Formation: Bacterial attachment and biofilm formation on microparticles and flat films were conducted as previously described[16] (Huesler et al.). Briefly, UV-sterilized 48-well plates with particles were incubated with RPMI medium (1 mL) and inoculated with a *P. aeruginosa* culture (OD_{600} of 0.01) for 24 h at 37 °C and with shaking at 60 rpm. Flat films were prepared by UV-polymerising the monomers EGDPEA and HPhOPA with 1% w/v photoinitiator (2,2 dimethoxy-2-phenylacetophenone) in an inert atmosphere (argon atmosphere <0.2% O_2) on glass coverslips. The coverslips had previously been activated through a silanization process using a solution of 3-(trimethoxysilyl)propyl methacrylate (2% w/v in dry toluene at 50 °C in an inert atmosphere for 24 h). Air-dried samples were examined using a Carl Zeiss LSM 700 laser scanning confocal microscope fitted with 555 nm excitation lasers and a 10×/NA 0.3 objective. Images were acquired using ZEN 2009 imaging software (Carl Zeiss) stacking these optical cross-sections acquired at different depths within a sample, a 3D image can be reconstructed. Bacterial surface coverage on microparticles was quantified using a MATLAB (R2016b) script on the fluorescence images (area size 568 × 568 µm, image resolution 512 × 512 pixels at 8-bit color depth) taken from each well while on flat films with COMSTAT.[32] However, fluorescence images representing an area of 295 × 295 µm with a resolution of 1024 × 1024 pixels at a 12-bit color depth were acquired on the microparticles, once transferred onto glass slides, to observe in depth the bacterial surface coverage.

Supporting Information

Supporting Information is available from the Wiley Online Library or from the author.

Acknowledgements

A.A.D. and V.C.C. contributed equally to this work. This work was supported by the Engineering and Physical Sciences Research Council [grant number EP/N0016615/1] and the Wellcome Trust [grant numbers 103882 and 103884]. All relevant data are available from the University of Nottingham's Research Data Management Repository.

Conflict of Interest

The authors declare no conflict of interest.

Keywords

biofilm prevention, catalytic chain transfer polymerisation, comb-graft polymers, droplet microfluidics, ToF-SIMS

Received: February 26, 2020
Revised: April 29, 2020
Published online: June 25, 2020

[1] V. Taresco, I. Louzao, D. Scurr, J. Booth, K. Treacher, J. Mccabe, E. Turpin, C. A. Laughton, C. Alexander, J. C. Burley, M. C. Garnett, *Mol. Pharmaceutics* **2017**, *14*, 2079.
[2] A. K. Patel, M. W. Tibbitt, A. D. Celiz, M. C. Davies, R. Langer, C. Denning, M. R. Alexander, D. G. Anderson, *Curr. Opin. Solid State Mater. Sci.* **2016**, *20*, 202.
[3] A. D. Celiz, A. L. Hook, D. J. Scurr, D. G. Anderson, R. Langer, M. C. Davies, M. R. Alexander, *Surf. Interface Anal.* **2013**, *45*, 202.
[4] E. P. Magennis, A. L. Hook, M. C. Davies, C. Alexander, P. Williams, M. R. Alexander, *Acta Biomater.* **2016**, *34*, 84.
[5] A. L. Hook, C.-Y. Chang, J. Yang, S. Atkinson, R. Langer, D. G. Anderson, M. C. Davies, P. Williams, M. R. Alexander, *Adv. Mater.* **2013**, *25*, 2542.
[6] L. K. Hansen, M. Brown, D. Johnson, D. F. Palme, C. Love, R. Darouiche, *Pacing Clin. Electrophysiol.* **2009**, *32*, 898.
[7] Y. Mei, K. Saha, S. R. Bogatyrev, J. Yang, A. L. Hook, Z. I. Kalcioglu, S.-W. Cho, M. Mitalipova, N. Pyzocha, F. Rojas, K. J. Van Vliet, M. C. Davies, M. R. Alexander, R. Langer, R. Jaenisch, D. G. Anderson, *Nat. Mater.* **2010**, *9*, 768.
[8] A. A. Dundas, O. Sanni, J. Dubern, G. Dimitrakis, A. L. Hook, D. J. Irvine, P. Williams, M. R. Alexander, *Adv. Mater.* **2019**, *31*, 1903513.
[9] O. Sanni, C. Y. Chang, D. G. Anderson, R. Langer, M. C. Davies, P. M. Williams, P. Williams, M. R. Alexander, A. L. Hook, *Adv. Healthcare Mater.* **2015**, *4*, 695.
[10] A. L. Hook, C.-Y. Chang, J. Yang, J. Luckett, A. Cockayne, S. Atkinson, Y. Mei, R. Bayston, D. J. Irvine, R. Langer, D. G. Anderson, P. Williams, M. C. Davies, M. R. Alexander, *Nat. Biotechnol.* **2012**, *30*, 868.
[11] A. Curtis, C. Wilkinson, *Biomaterials* **1997**, *18*, 1573.
[12] W. Teughels, N. Assche, I. Sliepen, M. Quirynen, *Clin. Oral Implants Rese.* **2006**, *17*, 68.
[13] M. Alvarez-Paino, M. H. Amer, A. Nasir, V. Cuzzucoli Crucitti, J. Thorpe, L. Burroughs, D. Needham, C. Denning, M. R. Alexander, C. Alexander, F. R. A. J. Rose, *ACS Appl. Mater. Interfaces* **2019**, *11*, 34560.
[14] C. Siltanen, M. Diakatou, J. Lowen, A. Haque, A. Rahimian, G. Stybayeva, A. Revzin, *Acta Biomater.* **2018**, *71*, 522.
[15] Q. Xu, M. Hashimoto, T. T. Dang, T. Hoare, D. S. Kohane, G. M. Whitesides, R. Langer, D. G. Anderson, H. David, *Small* **2009**, *5*, 1575.
[16] A. Hüsler, S. Haas, L. Parry, M. Romero, T. Nisisako, P. Williams, R. D. Wildman, M. R. Alexander, *RSC Adv.* **2018**, *8*, 15352.
[17] J.-C. Baret, *Lab Chip* **2012**, *12*, 422.
[18] C. Adlhart, J. Verran, N. F. Azevedo, H. Olmez, M. M. Keinänen-Toivola, I. Gouveia, L. F. Melo, F. Crijns, *J. Hosp. Infect.* **2018**, *99*, 239.
[19] G. Cheng, Z. Zhang, S. Chen, J. D. Bryers, S. Jiang, *Biomaterials* **2007**, *28*, 4192.
[20] A. A. Gridnev, S. D. Ittel, *Chem. Rev.* **2001**, *101*, 3611.
[21] J. P. A. Heuts, N. M. B. Smeets, *Polym. Chem.* **2011**, *2*, 2407.
[22] K. Adlington, N. T. Nguyen, E. Eaves, J. Yang, C. Y. Chang, J. Li, A. L. Gower, A. Stimpson, D. G. Anderson, R. Langer, M. C. Davies, A. L. Hook, P. Williams, M. R. Alexander, D. J. Irvine, *Biomacromolecules* **2016**, *17*, 2830.
[23] M. R. Alexander, P. Williams, *Biointerphases* **2017**, *12*, 02C201.
[24] J. D. Biasutti, G. E. Roberts, F. P. Lucien, *Eur. Polym. J.* **2003**, *39*, 429.
[25] S. Oliver, L. Zhao, A. J. Gormley, R. Chapman, C. Boyer, *Macromolecules* **2019**, *52*, 3.
[26] B. J. Tyler, A. Hook, A. Pelster, P. Williams, M. Alexander, H. F. Arlinghaus, *Biointerphases* **2017**, *12*, 02C412.
[27] J. Abdul, S. Salman, M. F. H. Kadhemy, *Int. J. Curr. Microbiol. Appl. Sci.* **2014**, *3*, 301.
[28] A. L. Hook, C.-Y. Chang, J. Yang, D. J. Scurr, R. Langer, D. G. Anderson, S. Atkinson, P. Williams, M. C. Davies, M. R. Alexander, *J. Vis. Exp.* **2012**, *59*, e3636.
[29] D. G. Anderson, S. Levenberg, R. Langer, *Nat. Biotechnol.* **2004**, *22*, 863.
[30] R. Popat, S. A. Crusz, M. Messina, P. Williams, S. A. West, S. P. Diggle, *Proc. R. Soc. B* **2012**, *279*, 4765.
[31] J. U. Izunobi, C. L. Higginbotham, *J. Chem. Educ.* **2011**, *88*, 1098.
[32] A. Heydorn, A. T. Nielsen, M. Hentzer, C. Sternberg, M. Givskov, B. K. Ersboll, S. Molin, *Microbiology* **2000**, *146*, 2395.